# Formation of Crystalline Nanoclusters of $Fe_2P$, RuP, $Co_2P$, $Rh_2P$, $Ni_2P$, $Pd_5P_2$, or $PtP_2$ in a Silica Xerogel Matrix from Single-Source Molecular Precursors

C. M. Lukehart* and Stephen B. Milne

*Department of Chemistry, Vanderbilt University, Nashville, Tennessee 37235*

S. R. Stock

*School of Materials Science and Engineering, Georgia Institute of Technology, Atlanta, Georgia 30332*

*Received October 14, 1997. Revised Manuscript Received December 29, 1997*

Metal complexes containing bifunctional phosphine ligands that possess alkoxysilyl functional groups have been prepared for seven metals of the first, second, or third transition metal series. Incorporation of these single-source precursors into silica xerogel matrixes using sol−gel chemistry affords molecularly doped xerogels. Subsequent thermal treatment of these doped xerogels under solely reducing conditions selectively affords nanoclusters of $Fe_2P$, RuP, $Co_2P$, $Rh_2P$, $Ni_2P$, $Pd_5P_2$, or $PtP_2$ which are highly dispersed throughout the bulk of the xerogel matrix. Characterization of these nanocomposite materials by transmission electron microscopy, energy-dispersive spectrometry, X-ray diffraction, and electron diffraction indicates that the metal phosphide nanoclusters are highly crystalline with some exhibiting nonspherical morphology.

## Introduction

Nanocomposite materials consisting of very small particles of a guest substance (typically having diameters less than 100 nm) dispersed throughout a host matrix are of intense current interest for potential applications in chemical catalysis and as magnetic, electronic, or photonic materials.[1−6] Recent interest in nanoparticulate III−V compounds or nanocomposites has included main group metal phosphides such as GaP or InP.[7] However, transition metals form a large class of metal phosphide compounds comprising over 125 binary and over 80 ternary substances differing in metal identity and metal/phosphorus stoichiometry.[8] Bulk band gap energies for most of these transition metal phosphides fall within the range of near 0 to over 3 eV, and many metal phosphides are technologically important as semiconductors or as phosphorescent, magnetic, or electronic materials.[8,9] Such a large class of substances having band gap energies typical of semiconductors represent prime candidates for study as new quantum dot materials. To our knowledge, such studies have not been reported on transition metal phosphides principally due to difficulties in preparing pure nanoparticulate materials. The overriding synthetic challenge is the preparation of crystalline transition metal phosphide nanoclusters of precise metal/phosphorus (M/P) stoichiometry.

Conventional syntheses of bulk metal phosphides usually involve direct reaction of the appropriate elements for prolonged periods at high temperature, reaction of phosphine with metals or metal oxides, reduction of metal phosphates by carbon, electrolysis of molten metal phosphate salts, chemical vapor deposition, or solid-state metathesis.[8−11] The main group metal phosphides, $Cd_3P_2$, $ZnGeP_2$, and $CdGeP_2$, have been prepared as powders from suitable molecular precursors,[12] while the transition metal phosphide, $Co_2P$, is formed along with Co metal when $[Co(CO)_3PEt_3]_2$ is subjected to thermogravimetric analysis.[13] Frequently, such traditional synthetic routes to metal phosphides give products of uncertain purity.

We now report a synthetic route to seven transition metal phosphide nanocomposites in which the host matrix is silica xerogel. Mono- or dinuclear transition metal phosphine complexes serve as single-source molecular precursors to metal phosphide nanoclusters. The silica xerogel host matrix is formed using conventional

* To whom correspondence should be addressed.

(1) Stucky, G. D. *Naval Res. Rev.* **1991**, *43*, 28.
(2) Sinfelt, J. H.; Meitzner, G. D. *Acc. Chem. Res.* **1993**, *26*, 1.
(3) Steigerwald, M. L.; Brus, L. E. *Acc. Chem. Res.* **1990**, *23*, 183.
(4) Wang, Y. *Acc. Chem. Res.* **1991**, *24*, 133.
(5) Weller, H. *Angew. Chem., Int. Ed. Engl.* **1993**, *32*, 41.
(6) Weller, H. *Adv. Mater.* **1993**, *5*, 88.
(7) Halanoui, L. I.; Kher, S. S.; Lube, M. S.; Aubuchon, S. R.; Hagan, C. R. S.; Wells, R. L.; Coury, L. A., Jr. *Nanotechnology: Molecularly Designed Materials*; Chow, G.-M., Gonsalves, K. E., Eds.; ACS Symposium Series 622; American Chemical Society: Washington, DC, 1996; p 178.
(8) von Schnering, H. G.; Honle, W. *Encyclopedia of Inorganic Chemistry*; John Wiley & Sons: Chichester, U.K., 1994; Vol. 6, p 3106.
(9) Arinsson, B.; Landstrom, T.; Rundquist, S. *Borides, Silicides and Phosphides*; Wiley: New York, 1965.
(10) Hector, A. L.; Parkin, I. P. *J. Mater. Chem.* **1994**, *4*, 279.
(11) (a) Parkin, I. P. *Chem. Soc. Rev.* **1996**, 199. (b) Gopalakrishnan, J.; Pandey, S.; Rangan, K. K. *Chem. Mater.* **1997**, *9*, 2113.
(12) Goel, S. C.; Chiang, M. Y.; Buhro, W. E. *J. Am. Chem. Soc.* **1990**, *112*, 5636.
(13) Gross, M. E.; Lewis, J. *J. Vac. Sci. Technol. B* **1988**, *6*, 1553.

S0897-4756(97)00673-X CCC: $15.00 
Published on Web 02/25/1998

sol−gel chemistry. Each molecular precursor has at least one bifunctional phosphine ligand containing a $Si(OR)_3$ functional group, thereby ensuring homogeneous, covalent incorporation of the precursor into the silica xerogel matrix as it is being formed. Subsequent thermal treatment of these molecularly doped xerogels under reducing conditions gives silica xerogels containing nanoparticulate metal phosphides. Thermal conditions are chosen such that these metal phosphide nanoclusters are formed with sufficient size and crystallinity to permit characterization by diffraction methods. Metal phosphide/silica xerogel nanocomposites containing nanoclusters of $Fe_2P$, RuP, $Co_2P$, $Rh_2P$, $Ni_2P$, $Pd_5P_2$, or $PtP_2$ have been prepared using this strategy. Selective formation of a specific metal phosphide composition for each metal is an unexpected and fortuitous result. An overview of nanocomposite syntheses using this general synthetic strategy has been reported recently.[14]

## Experimental Section

**Reagents and Methods.** Tetramethyl orthosilicate (TMOS) was purchased from Aldrich Chemical Co., Inc. Diphenylphosphine, diethylphosphine, bis($\eta^4$-1,5-cyclooctadiene)nickel, ($\eta^4$-1,5-cyclooctadiene)platinum(II) chloride, and iron pentacarbonyl were purchased from Strem Chemical Company, Inc. Vinyltrimethoxysilane and vinyltriethoxysilane were purchased from Huls America, Inc. α-Phellandrene was acquired from Pfaltz and Bauer, Inc. The bifunctional phosphines, $Ph_2PCH_2CH_2Si(OCH_3)_3$, $L^A$, $Ph_2PCH_2CH_2Si(OEt)_3$, $L^B$, and $Et_2PCH_2CH_2Si(OEt)_3$, $L^C$, were prepared according to literature procedures.[15] Reactions were performed in oven-dried glassware under a nitrogen or argon atmosphere. Tetrahydrofuran (THF), hexane, or ether were purified by distillation from sodium/benzophenone. Methylene chloride was dried by distillation from calcium hydride. Benzene was purified by distillation from sodium. Other solvents and reagents were used without further purification.

Silica xerogels were formed at 25 °C using standard sol−gel formulations with minor modification of the procedure reported by Sakka.[16,17] All operations were performed at room temperature unless otherwise specified. Microanalyses were performed by Galbraith Laboratories, Inc., Knoxville, TN, or by Oneida Research Services, Inc., Whitesboro, NY.

$^1$H-, $^{13}$C-, or $^{31}$P-NMR spectra were recorded on a IBM NR-300 spectrometer operating at 300, 75, or 121 MHz, respectively, using the $^2$H signal of the solvent as an internal lock frequency. Chemical shifts (in $\delta$) were measured for $^1$H-NMR and $^{13}$C-NMR spectra relative to tetramethylsilane using the residual solvent peak as an internal standard while chemical shifts (in $\delta$) were measured for $^{31}$P-NMR spectra relative to an external standard of 85% $H_3PO_4$ with positive values being downfield of the respective references.

Nanocomposite materials were characterized by using a Philips CM20T transmission electron microscope operating at 200 kV. Samples for transmission electron microscopy (TEM) were prepared by dispersing a powdered sample of nanocomposite onto a 3-mm diameter copper grid covered with amorphous carbon as a substrate. These samples were analyzed with standard bright-field (BF) imaging for particle-size distribution, selected area diffraction (SAD) for their crystal structures, and X-ray energy dispersive spectroscopy (EDS) for semiquantitative chemical composition.

X-ray diffraction (XRD) scans were obtained using a Philips PW1800 $\theta/2\theta$ automated powder diffractometer equipped with a Cu target and a post-sample monochromator. Samples for XRD were prepared by placing a uniform layer of powdered nanocomposite onto double-sided tape affixed to the sample holder. The sample area was greater than the ca. 1 cm × 1 cm area irradiated by the X-ray beam. Considerable caution was used to keep the top of the sample surface flat and coplanar with the diffractometer rotation axis. Prior to peak width measurement, each diffraction peak was corrected for background scattering and was stripped of the $K\alpha_2$ portion of the diffracted intensity. The full width at half-maximum (fwhm) was measured for each selected peak. Crystallite size, $L$, was calculated from Scherrer's equation, ($L = K\lambda/(\beta \cos \theta_B)$), for peak broadening from size effects only (where $\beta$ is the peak fwhm measured in radians on the $2\theta$ scale, $\lambda$ is the wavelength of X-rays used, $\theta_B$ is the Bragg angle for the measured $hkl$ peak, and $K$ is a constant equal to 1.00 for $L$ taken as the volume-averaged crystallite dimension perpendicular to the $hkl$ diffraction plane).[18]

The typical process used for identification of each metal phosphide substance is represented best for the nickel phosphide/silica xerogel nanocomposite because the number of documented nickel phosphide substances is the largest of the metal phosphides described in this work. Powder XRD data for the nickel phosphide/silica xerogel nanocomposite was compared with those data listed for the 10 different nickel phosphide cards contained in the Powder Diffraction File and revealed that only the substance $Ni_2P$ (card no. 3-953) was a viable identification. Both the $d$-spacings and the relative intensities were consistent with this phase, and phase identification software provided with the diffractometer system identified $Ni_2P$ (card no. 3-953) and no other phases as containing the elements present in the synthesis. The values of $d$-spacings obtained from the $Ni_2P$/silica xerogel nanocomposite were within 0.01 Å of those listed for $Ni_2P$ as a pure substance (card no. 3-953).

**Syntheses of Molecular Precursors 1a−7a. Preparation of Tetracarbonyl{diphenyl[2-(trimethoxysilyl)ethyl]phosphine}iron(0), 1a.** To a stirred solution of diphenyl[2-(trimethoxysilyl)ethyl]phosphine, $L^A$ (1.00 g, 2.65 mmol), in cyclohexane (5 mL) was added iron pentacarbonyl (0.586 g, 2.99 mmol) in a quartz reaction tube. The resulting mixture was then irradiated with an ultraviolet lamp for 16 h, yielding a deep red-orange solution. Solvents were removed at reduced pressure yielding **1a** as a deep red-orange oil (0.874 g, 58% yield): $^1$H-NMR ($CDCl_3$) $\delta$ 7.57 (m, 4H, aromatic), 7.45 (m, 6H, aromatic), 3.53 (s, 9H, $OCH_3$), 2.52 (m, 2H, $PCH_2$), 0.85 (m, 2H, $CH_2Si$); $^{31}$P[$^1$H]-NMR ($CDCl_3$) $\delta$ +68.80 (s); $^{13}$C[$^1$H]-NMR ($CDCl_3$) $\delta$ 213.10 (d, $^2J_{PC}$ = 19.0 Hz, $C$=O), 133.50 (d, $^1J_{PC}$ = 47.0 Hz, aromatic, $C_1$), 131.80 (d, $^3J_{PC}$ = 9.00 Hz, aromatic, $C_3$), 130.50 (s, aromatic, $C_4$), 128.40 (d, $^3J_{PC}$ = 10.0 Hz, aromatic, $C_2$), 50.39 (s, $OCH_3$), 26.02 (d, $^1J_{PC}$ = 28.0 Hz, $CH_2P$), 3.33 (s, $CH_2Si$). Anal. Calcd for $C_{21}H_{23}FeO_7PSi$: C, 50.21; H, 4.62; P, 6.17. Found: C, 49.93; H, 4.76; P, 6.21.

**Preparation of ($\eta^6$-*p*-Cymene)dichloro{diphenyl[2-(triethoxysilyl)ethyl]phosphine}ruthenium(II), 2a.** Following an analogous preparation reported by Bennett and coworkers,[19] ruthenium trichloride (1.60 g, 7.70 mmol) and α-phellandrene (8.38 g, 61.5 mmol) in ethanol (100 mL) were refluxed for 4 h, yielding di-$\mu$-chloro-bis[chloro($\eta^6$-*p*-cymene)-ruthenium(II)]. This dimer (0.372 g, 0.601 mmol) was dissolved in $CH_2Cl_2$ (25 mL), forming an orange solution. To this solution was added dropwise diphenyl[2-(triethoxysilyl)ethyl]-phosphine, $L^B$ (0.458 g, 1.22 mmol). After the solution was stirred for 2 h, the solvents were removed, yielding a brown solid. Recrystallization from $CH_2Cl_2$/pentane solution afforded **2a** as a red-brown solid (0.465 g, 56.0% yield): mp 130−133

(14) Carpenter, J. P.; Lukehart, C. M.; Milne, S. B.; Stock, S. R.; Wittig, J. E.; Jones, B. D.; Glosser, R.; Henderson, D. O.; Mu, R.; Shull, R. D.; Zhu, J. G.; Rek, Z. U. *SAMPE Technol. Conf.* **1995**, *27*, 549.
(15) Niebergall, H. *Makromol. Chem.* **1962**, *59*, 218.
(16) Brinker, C. J.; Scherer, G. W. *Sol-Gel Science*; Academic Press: New York, 1990.
(17) Adachi, T.; Sakka, S. *J. Mater. Sci.* **1987**, *22*, 4407.
(18) (a) Klug, H. P.; Alexander, L. E. *X.-Ray Diffraction Procedures for Polycrystalline and Amorphous Materials*, 2nd ed.; John Wiley & Sons: New York, 1974. (b) Halpwerin, W. P. *Rev. Mod. Phys.* **1986**, *58*, 533.
(19) Bennett, M. A.; Smith, A. K. *J. Chem. Soc., Dalton Trans.* **1974**, 233.

**Table 1. Preparative Details and Analysis of Molecularly Doped Silica Xerogels[a]**

| | $Fe_2P$, **1b** | RuP, **2b** | $Co_2P$, **3b** | $Rh_2P$, **4b** | $Ni_2P$, **5b** | $Ni_2P$, **5b′** | $Pd_5P_2$, **6b** | $PtP_2$, **7b** |
|---|---|---|---|---|---|---|---|---|
| precursor, $\mu$mol | **1a**, 313 | **2a**, 68 | **3a**, 78 | **4a**, 320 | **5a**, 10 | **5a′**, 159 | **6a**, 141 | **7a**, 115 |
| TMOS (mmol) | 3.13 | 0.68 | 2.35 | 3.20 | 0.10 | 1.59 | 1.41 | 5.73 |
| mole ratio Si/M | 11 | 11 | 16 | 13 | 14 | 12 | 12 | 52 |
| water (mmol) | 31.3 | 6.8 | 23.5 | 32 | 1 | 15.9 | 14 | 57.3 |
| methanol (mL) | 5 | 5 | 5 | 5 | 1 | 5 | 5 | 0 |
| cosolvent | DMF | DMF | DMF | DMF | DMF | DMF | DMF | THF |
| volume (mL) | 0.23 | 0.05 | 0.15 | 0.24 | 0.01 | 0.10 | 0.10 | 5.0 |
| color | orange | orange | purple | orange | white | pale green | yellow | amber |
| xerogel mass (mg) | 272 | 70 | 288 | 542 | 27 | 275 | 218 | 923 |
| wt % of metal | 4.20 | 6.69 | 3.25 | 4.03 | 2.58 | 2.18 | 17.15 | 1.77[b] |
| wt % of Si | 27.38 | 21.62 | 21.76 | 19.02 | 19.94 | 15.51 | 22.64 | 27.56[b] |
| wt % of P | 2.44 | 1.54 | 1.71 | 4.76 | 4.25 | 2.10 | 8.69 | 1.00[b] |
| mole ratio Si/M | 13.0 | 11.6 | 14.1 | 17.3 | 16.2 | 14.9 | 5.0 | 108[b] |
| mole ratio M/P | 0.95 | 1.33 | 1.00 | 0.25 | 0.32 | 0.54 | 0.57 | 0.29[b] |

[a] Catalyst: 0.02 mL of 0.148 M aqueous $NH_3$. [b] Data determined on a sample prepared using a Si/Pt reagent molar ratio of 80.5.

°C; $^1$H-NMR ($CDCl_3$) $\delta$ 7.86 (m, 4H, aromatic), 7.46 (m, 6H, aromatic), 5.24 (d, $^3J_{HH}$ = 5.64 Hz, 2H, arene), 5.06 (d, $^3J_{HH}$ = 5.64 Hz, 2H, arene), 3.67 (q, $^3J_{HH}$ = 6.97 Hz, 6H, $OCH_2CH_3$), 2.66 (m, 2H, $PCH_2$), 2.55 (sept, $^3J_{HH}$ = 6.95 Hz, 1H, $CH(CH_3)_2$), 1.88 (s, 3H, $CH_3$), 1.12 (t, $^3J_{HH}$ = 6.97 Hz, 9H, $OCH_2CH_3$), 0.82 (d, $^3J_{HH}$ = 6.95 Hz, 6H, $CH(CH_3)_2$), 0.35 (m, 2H, $SiCH_2$); $^{31}$P-[$^1$H]-NMR ($CDCl_3$) $\delta$ +26.07 (s); $^{13}$C[$^1$H]-NMR ($CDCl_3$) $\delta$ 133.40 (d, $^3J_{PC}$ = 8.37 Hz, aromatic, $C_3$), 132.50 (d, $^1J_{PC}$ = 41.86 Hz, aromatic, $C_1$), 130.40 (s, aromatic, $C_4$), 128.20 (d, $^2J_{PC}$ = 9.31 Hz, aromatic, $C_2$), 108.10 (s, arene, $C_1$ or $C_4$), 93.50 (s, arene, $C_1$ or $C_4$), 90.50 (s, arene, $C_2$ or $C_3$), 85.40 (s, arene, $C_2$ or $C_3$), 58.50 (s, $OCH_2CH_3$), 29.90 (s, $CH(CH_3)_2$), 21.30 (s, $CH(CH_3)_2$), 18.20 (s, $OCH_2CH_3$), 17.25 (m, $PCH_2$ and $CH_3$), 3.40 (d, $^2J_{PC}$ = 9.00 Hz, $SiCH_2$). Anal. Calcd for $C_{30}H_{43}Cl_2O_3PRuSi$: C, 52.77; H, 6.36; P, 4.54. Found: C, 52.24; H, 6.24; P, 4.52.

**Preparation of Hexacarbonyl{diphenyl[2-(triethoxysilyl)ethyl]phosphine}dicobalt(0), 3a.** Complex **3a** was prepared according to the procedure reported by Schubert and co-workers.[20]

**Preparation of Chlorotris{diethyl[2-(triethoxysilyl)ethyl]phosphine}rhodium(I), 4a.** To a stirred solution of $\mu,\mu'$-dichlorobis[($\eta^4$-1,5-cyclooctadiene)dirhodium(I)[21] (0.189 g, 0.384 mmol) in benzene (10 mL) was added dropwise diethyl-[2-(triethoxysilyl)ethyl]phosphine, $L^C$ (0.650 g, 2.30 mmol). After 20 h of reaction, the solvent was removed at reduced pressure and pentane was added. Cooling the resulting solution afforded **4a** as a deep red oil (0.611 g, 73.1% yield): $^1$H-NMR ($CDCl_3$) $\delta$ 3.83 (q, $^3J_{HH}$ = 6.92 Hz, 6H, $OCH_2CH_3$), 1.98 (m, 6H, $PCH_2CH_2$ and $PCH_2CH_3$), 1.22 (t, $^3J_{HH}$ = 6.92 Hz, 9H, $OCH_2CH_3$), 1.15 (m, 6H, $PCH_2CH_3$), 0.825 (m, 2H, $PCH_2CH_2Si$); $^{31}$P[$^1$H]-NMR ($CDCl_3$) $\delta$ +26.11 (d of t, $^1J_{RhP}$ = 149 Hz, $^2J_{PP}$ = 26.5 Hz), +14.99 (d of d, $^1J_{RhP}$ = 93.6 Hz, $^2J_{PP}$ = 26.5 Hz). Anal. Calcd for $C_{36}H_{87}ClO_9P_3RhSi_3$: C, 44.13; H, 8.95. Found: C, 43.60; H, 8.30.

**Preparation of Tetrakis{diphenyl[2-(triethoxysilyl)ethyl]phosphine}nickel(0), 5a.** A solution of diphenyl[2-(triethoxysilyl)ethyl]phosphine, $L^B$ (0.438 g, 1.16 mmol), in hexane (5 mL) was added at 0 °C to a flask containing bis($\eta^4$-1,5-cyclooctadiene)nickel(0) (0.080 g, 0.29 mmol). The resulting orange-red solution was allowed to slowly warm to room temperature over 4 h. At this point, the solution was again cooled to 0 °C, and pentane was added. The off-white precipitate was filtered, rinsed with hexane and ether, and dried at reduced pressure to yield **5a** as a white solid (0.3752 g, 82% yield): mp 60−63 °C; $^{31}$P[$^1$H]-NMR ($CDCl_3$) $\delta$ +32.01 (s); $^1$H-NMR ($CDCl_3$) $\delta$ 7.74 (m, 4H, aromatic), 7.48 (m, 6H, aromatic), 3.78 (q, $^3J_{HH}$ = 6.87 Hz, 9H, $OCH_2CH_3$), 2.29 (m, 2H, $PCH_2$), 1.19 (t, $^3J_{HH}$ = 6.87 Hz, 6H, $OCH_2CH_3$), 0.85 (m, 2H, $CH_2Si$). Oxidaton by air converted the phosphine ligands into the corresponding phosphine oxide, as confirmed by NMR and by analysis. Anal. Calcd for $C_{80}H_{116}NiO_{16}P_4Si_4$: C, 58.99; H, 7.18. Found: C, 58.42; H, 7.17.

**Preparation of *trans*-[Bis{diphenyl[2-(triethoxysilyl)-ethyl]phosphine}nickel(II) Chloride], 5a′.** Complex **5a′** was prepared according to the procedure reported by Bemi and co-workers.[22]

**Preparation of Dibromobis{diethyl[2-(triethoxysilyl)-ethyl]phosphine}palladium, 6a.** ($\eta^4$-1,5-Cyclooctadiene)-palladium(II) bromide[23] (1.00 g, 2.67 mmol) was dissolved in $CH_2Cl_2$ (20 mL), yielding a deep red-orange solution. To this solution was added dropwise diethyl[2-(triethoxysilyl)ethyl]-phosphine, $L^C$ (1.49 g, 5.43 mmol). After the solution was stirred for 24 h, the solvent was removed by distillation. The resulting solid was recrystallized from $CH_2Cl_2$/pentane at −20 °C. Crystals were collected at −78 °C by removing solvents via syringe and drying under high vacuum to yield **6a** (1.31 g, 59.1% yield): mp 66−69 °C; $^{31}$P[$^1$H]-NMR ($CDCl_3$) $\delta$ 15.07 (s, cis, 90%), 16.85 (s, trans, 10%); $^1$H-NMR ($CDCl_3$) $\delta$ 3.84 (q, $^3J_{HH}$ = 6.98 Hz, 6H, $OCH_2CH_3$), 2.02 (m, 6H, $PCH_2CH_2$ and $PCH_2CH_3$), 1.24 (t, $^3J_{HH}$ = 6.98 Hz, 9H, $OCH_2CH_3$), 1.12 (m, 6H, $PCH_2CH_3$), 0.82 (m, 2H, $PCH_2CH_2Si$); $^{13}$C[$^1$H]-NMR ($CDCl_3$) $\delta$ 58.58 (s, $OCH_2CH_3$), 18.30 (s, $OCH_2CH_3$), 15.49 (m, $PCH_2$-$CH_2$ & $PCH_2CH_3$), 8.27 (s, $CH_2CH_3$), 4.39 (s, $SiCH_2$). Anal. Calcd for $C_{24}H_{58}Br_2O_6P_2PdSi_2$: C, 34.85; H, 7.08; P, 7.49. Found: C, 34.02; H, 6.69; P, 7.70.

**Preparation of Dichlorobis{diphenyl[2-(trimethoxysilyl)ethyl]phosphine}platinum(II), 7a.** To a solution of ($\eta^4$-1,5-cyclooctadiene)platinum(II) chloride (1.00 g, 2.69 mmol) in 40 mL of methylene chloride was added dropwise a solution of $Ph_2PCH_2CH_2Si(OCH_3)_3$ (1.80 g, 5.38 mmol) in 5 mL of methylene chloride. The reaction solution became yellow but quickly faded to a clear, colorless solution. After 2 h, the solvent was removed at reduced pressure to concentrate the reaction solution to 5 mL, and 50 mL of hexane was added to precipitate a white solid. The resulting mixture was stored at −30 °C for 16 h. The white precipitate was then isolated by filtration, was washed with 3 × 10 mL of hexane, and was dried at reduced pressure to give 2.19 g (87% yield) of the product. Recrystallization of this product from methylene chloride/hexane solution at −30 °C afforded **7a** as white needles: mp 180−181° C; $^1$H-NMR ($CDCl_3$) $\delta$ 0.80 (m, 4H, $SiCH_2$), 2.35 (m, 4H, $PCH_2$), 3.43 (s, 18H, $OCH_3$), 7.10−7.55 (m, 20H, $PPh$); $^{31}$P{$^1$H}-NMR ($CDCl_3$) $\delta$ 9.26 (s, 1, $^1J_{PtP}$ = 3662 Hz). Anal. Calcd for $C_{34}H_{46}Cl_2O_6P_2PtSi_2$: C, 43.68; H, 4.96. Found: C, 43.57; H, 5.10.

**Syntheses of Molecularly Doped Silica Xerogels 1b−7b.** Conventional sol−gel formulations were followed[16] for the synthesis of silica xerogels containing covalent incorporation of molecular precursors using modifications similar to those reported by Sakka.[17] Preparative details for each synthesis are shown in Table 1. All silica xerogels were formed at room temperature in plastic vials by hydrolysis of TMOS using aqueous ammonia as catalyst. Due to the air sensitivity of precursor **5a**, xerogel **5b** was prepared successfully under

(20) Schubert, U.; Rose, K.; Schmidt, H. *J. Non-Cryst. Solids* **1988**, *105*, 165.
(21) Chatt, J.; Venanzi, L. M. *J. Chem. Soc.* **1957**, 4735.
(22) Bemi, L.; Clark, H. C.; Davies, J. A.; Fyfe, C. A.; Wasylishen, R. E. *J. Am. Chem. Soc.* **1982**, *104*, 438.
(23) Drew, D.; Doyle, J. R. *Inorg. Synth.* **1972**, *13*, 47.

**Table 2. Conditions for the Preparation of Metal Phosphide/Silica Xerogel Nanocomposites**

| | $Fe_2P$, **1c** | RuP, **2c** | $Co_2P$, **3c** | $Rh_2P$, **4c** | $Ni_2P$, **5c** | $Ni_2P$, **5c′** | $Pd_5P_2$, **6c** | $PtP_2$, **7c** |
|---|---|---|---|---|---|---|---|---|
| precursor, mg | **1b**, 272 | **2b**, 70 | **3b**, 152 | **4b**, 249 | **5b**, 7.6 | **5b'**, 137 | **6b**, 108 | **7b**, 640 |
| heat ($H_2$) *t*, *T* (°C) | 0.5 h, 900 | 2 h, 700 | 2 h, 800 | 2 h, 700 | 3 h, 750 | 3 h, 750 | 2 h, 600 | 2 h, 700 |
| final mass (mg) | 149 | 49 | 86 | 106 | 2.1 | 63 | 70 | 286 |
| color | red-blk | red-blk | black | red-blk | red-blk | black | black | black |
| wt % of metal | 5.82 | 11.03 | 3.09 | 6.62 | 5.10 | 6.06 | 10.21 | 2.30[c] |
| wt % of Si | 41.33 | 34.60 | 40.28 | 33.57 | 35.61 | 39.07 | 36.54 | 39.93[c] |
| wt % of P | 2.48 | 3.85 | 0.90 | 5.03 | 3.79 | 4.76 | 1.94 | 1.15[c] |
| mole ratio Si/M | 14.1 | 11.3 | 27.6 | 18.6 | 14.6 | 13.5 | 14.0 | 121[c] |
| mole ratio M/P | 1.30 | 0.88 | 1.79 | 0.40 | 0.71 | 0.67 | 1.53 | 0.32[c] |
| av diam (TEM, nm) | 4.7 | 4.7 | 5.0 | 2.0 | 2.6 | 35.5 | 11.3 | 4.0 |
| av diam (XRD, nm) | 10 | 5 | *b* | *a* | 9 | na | 13 | 5 |

[a] XRD peaks too broad for accurate particle size measurement. [b] Peak overlap prevents average particle size determination from peak widths. [c] Data determined on a sample prepared using a Si/Pt reactant molar ratio of 80.5.

nitrogen atomosphere using degassed solvents. The molar ratio of total water to TMOS was fixed at 10 with cosolvents being used to provide a solution of all reactants. Molar ratios of total silicon to metal ranged from 11 to 52. After addition of the specified catalyst, gels were aged at room temperature for 16−48 h. Wet xerogels were fractured, washed with methanol, and air-dried for at least 16 h. Solvent washings from preparations using colored precursors indicated essentially complete incorporation of precursor molecules within the xerogel. Evaporated wash solutions did not produce detectable amounts of precursor residue.

**Preparation of Metal Phosphide/Silica Xerogel Nanocomposites 1c−7c from Molecularly Doped Silica Xerogels.** The preparation of each metal phosphide/silica xerogel nanocomposite was performed using the same general procedure. A sample of a molecularly doped xerogel (prepared as described above) was ground to a powder and was then placed into an alumina boat (Fisher brand Combax). The alumina boat containing the sample was inserted into a quartz tube which was then placed into a Hoskins tube furnace. The atmosphere within the quartz tube was controlled by passing hydrogen gas through the tube at a rate of 150 mL per min, and the temperature of the sample was measured via an internal thermocouple placed directly above the sample. The temperature of the system was ramped to the stated reaction temperature over 1 h. Following thermal treatment, samples were cooled to room temperature over ca. 2 h.

Specific procedures for the preparation of each nanocomposite are provided in Table 2. The thermal conditions reported gave metal phosphide nanoclusters of sufficient size and crystallinity to be characterized by diffraction methods. The metal phosphide nanocluster loading was high enough to produce deeply colored nanocomposites.

**Preparation of Silica Xerogel with Incorporation of Diphenyl[2-(triethoxysilyl)ethyl]phosphine and Subsequent Thermal Treatment.** Phosphine $L^B$ (0.357 g, 0.948 mmol), TMOS (0.361 g, 2.37 mmol), *N*,*N*-dimethylformamide (0.170 g, 2.37 mmol), $H_2O$ (0.430 g, 23.7 mmol), and 0.148 M ammonia (0.03 mL, 0.004 mmol) were dissolved in methanol (3 mL) to initiate sol−gel conversion to silica xerogel. The resulting clear, colorless xerogel was rinsed with methanol and was air-dried to give 0.218 g of dry xerogel. When the phosphine-doped xerogel thus obtained (0.218 g) was heated in a hydrogen atmosphere for 3 h at 750 °C, 0.0730 g of off-white silica xerogel were obtained. Anal. Found: Si, 47.55; P, 1.35.

## Results

Metal phosphide/silica xerogel nanocomposites **1c**−**7c** have been prepared from molecular precursors (**1a**−**7a**) as shown in Scheme 1. These overall syntheses require three steps: (1) preparation of a single-source molecular precursor complex containing a bifunctional phosphine ligand, (2) covalent incorporation of these molecular precursors into a silica xerogel matrix as it is being formed, and (3) a thermal treatment that transforms the molecularly doped xerogel host matrix into a metal phosphide/silica xerogel nanocomposite.

**Scheme 1**

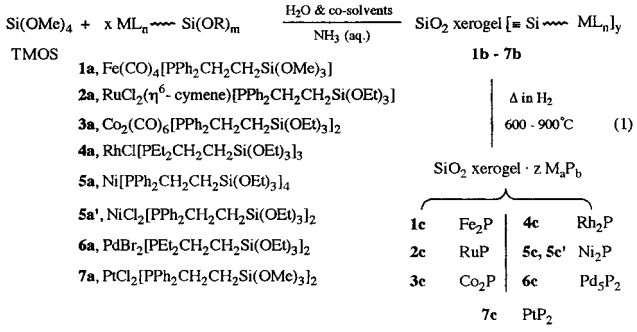


**Molecular Precursors 1a−7a.** Covalent incorporation of molecular precursors into a silica xerogel matrix as the matrix is being formed is accomplished by preparing molecular precursors which contain alkoxysilyl functional groups that can participate in sol−gel hydrolysis and condensation reactions. Molecular precursor complexes should also have adequate solubility and chemical stability to survive sol−gel conversion without undergoing chemical degradation.

Incorporation of bifunctional ligands into a molecular precursor is best accomplished as a final step in precursor synthesis. Synthetic strategies represented in the syntheses of precursors **1a**−**7a** are (1) direct displacement of carbonyl ligands by $PPh_2(CH_2)_2Si(OMe)_3$, $L^A$, or $PPh_2(CH_2)_2Si(OEt)_3$, $L^B$, giving precursors **1a** and **3a**, respectively; (2) cleavage of metal−halide dimers by the phosphines, $L^B$, or $PEt_2(CH_2)_2Si(OEt)_3$, $L^C$, to form the monomeric phosphine complexes, **2a** and **4a**; (3) displacement of $\eta^4$-cyclooctadiene ligands by the bifunctional phosphines, $L^A$, $L^B$, or $L^C$, affording complexes **4a**, **5a**, **6a**, or **7a**; and (4) displacement of a weakly coordinated aquo ligand by the phosphine $L^B$, affording **5a′**.

**Molecularly Doped Silica Xerogels 1b−7b.** Silica xerogels containing covalent incorporation of each molecular precursor have been prepared using modified, though conventional, sol−gel formulations.[16,17] Details of these preparations are provided in Table 1. Choice of cosolvent is determined by the solubility properties of the precursor complex. All of these nanocomposites can be prepared using loading levels of molecular precursor different from those conditions listed in Table 1.

Covalent incorporation of precursors **1a**−**7a** into a silica xerogel matrix as it is being formed is supported by much previous work, as reported by Schubert,[24,25] Evans and Gracey,[26] and this laboratory.[27] EDS spectra of representative molecularly doped xerogels over multiple locations do not show significant variation in

relative amounts of silicon and metal, thus indicating uniform incorporation of precursor at least on the micrometer scale. Furthermore, essentially all of the precursor complex is retained within the xerogel and cannot be extracted from the matrix by solvent washing. A related control study confirming this observation has been reported.[27] In all cases, the ceramic yield of silica xerogel in nanocomposites **1b**−**7b** is at least 72%.

**Metal Phosphide/Silica Xerogel Nanocomposites 1c**−**7c.** Metal phosphide/silica xerogel nanocomposites are prepared directly upon thermal treatment of the molecularly doped xerogels **1b**−**7b** under a reducing atmosphere. Specific conditions for each thermal treatment are provided in Table 2. These conditions afford metal phosphide nanoclusters of sufficient size and crystallinity to permit characterization by diffraction methods. Each dopant complex acts as a single-source molecular precursor for only one metal phosphide composition (vide infra).

Chemical microanalytical data for these nanocomposites reveal consistently high silicon content as expected for metal phosphide/$SiO_2$ compositions. Metal retention of 90% or higher is observed following reductive thermal treatment for all nanocomposites except **3c** and **6c**. Significant metal loss occurs during the thermal treatment of **3b** (49% loss) and **6b** (64% loss) probably owing to the loss of volatile compounds containing metal. The mechanism by which this loss of metal occurs has not been studied. M/P molar ratios reveal a phosphorus content greater than that required by the metal phosphide stoichiometry. Because on-particle EDS measurements typically indicate M/P atomic ratios consistent with the $M_aP_b$ stoichiometry, as confirmed by electron and X-ray diffraction, excess phosphorus is presumably incorporated into the silica xerogel matrix. However, microanalysis also indicates some phosphorus loss during thermal treatment. Volatile byproducts, including phosphorus compounds, formed during thermal treatment have not been isolated or identified.

The crystalline metal phosphide nanoclusters have been characterized by TEM, XRD, electron diffraction, and EDS. Representative TEM micrographs of each metal phosphide/silica xerogel nanocomposite are provided as Supporting Information. Although nanoclusters of nearly spheriodal shape are commonly observed, nanocrystals of $Fe_2P$ have striking hexagonal shapes (see Figure 1), giving a nanocluster morphology that reflects the hexagonal unit cell symmetry of this material. Histograms of metal phosphide particle sizes for nanocomposites **1c**−**7c** are also included as Supporting Information and reveal monomodal size distributions. Powder XRD scans of each nanocomposite are provided as Supporting Information along with patterns of the appropriate bulk metal phosphide. Although the X-ray structure of RuP has been published,[28] the powder pattern of this substance is not available within the ICDD powder diffraction file. The pattern provided for RuP was obtained using a modified Rietveld refinement procedure.[29] Selected area electron diffraction data and EDS scans of each nanocomposite are also included as Supporting Information. From three to nine *d*-spacings expected for the appropriate crystalline metal phosphide have been determined from observed ring patterns. Electron diffraction from a single $Fe_2P$ particle gives a spot pattern that can be successfully indexed using the unit cell parameters of barringerite. The absence of X-ray emissions from Cl or Br in the EDS spectra of the nanocomposites **2c**, **4c**, and **5a′**−**7a** indicates that thermal decomposition of the corresponding precursor complexes is essentially complete.

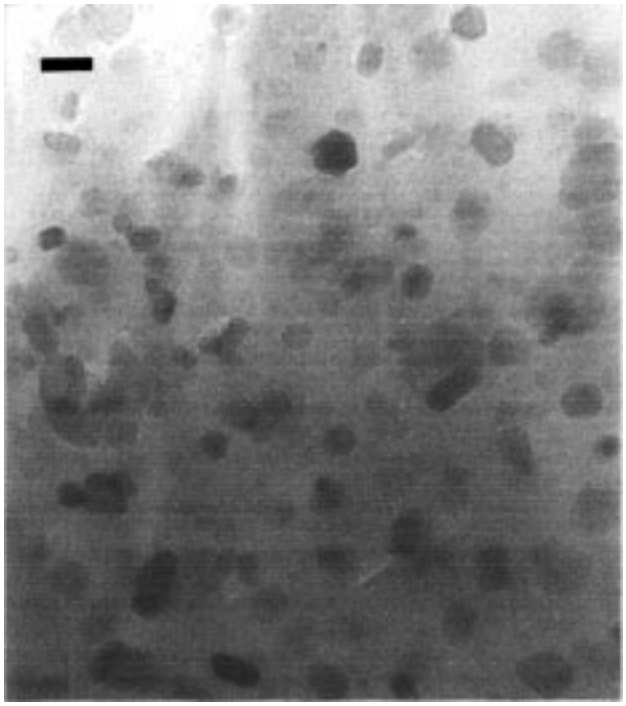

**Figure 1.** TEM micrograph of the $Fe_2P$/silica xerogel nanocomposite **1c** showing the nearly hexagonal morphology of the $Fe_2P$ nanocrystals (bar = 10 nm).

Average values of metal phosphide particle diameters for these seven nanocomposites range from 2.0 to 11.3 nm by TEM and from 5 to 13 nm by XRD (excluding nanocomposite **5c′**). Abnormally large $Ni_2P$ particles having average diameters of 35.5 nm (by TEM) are observed for nanocomposite **5c′**. The reason nanocomposite **5c′** affords $Ni_2P$ particles on average 14 times larger than those of **5c** when using the same molecular molar doping level and subsequent thermal treatment conditions is not evident. The close agreement of average metal phosphide particle size by TEM and XRD for nanocomposites **2c**, **6c**, and **7c** indicate that very few exceptionally large particles of RuP, $Pd_5P_2$, or $PtP_2$ are present in these samples.

## Discussion

Thermal treatment of the molecularly doped silica xerogels **1b**−**7b** under reducing conditions leads to the

(24) Breitscheidel, B.; Zieder, J.; Schubert, U. *Chem. Mater.* **1991**, *3*, 559.
(25) Schubert, U. *New J. Chem.* **1994**, *18*, 1049.
(26) Evans, J.; Gracey, B. P. *J. Chem. Soc., Dalton Trans.* **1982**, 1123.
(27) Carpenter, J. P.; Lukehart, C. M.; Stock, S. R.; Wittig, J. E. *Chem. Mater.* **1995**, *7*, 201.
(28) Rundqvist, S. *Acta Chem. Scand.* **1962**, *16*, 287.

(29) The XRD pattern for RuP was calculated from published structural data[28] using DBWS-9411 which is an upgrade of the DBWS programs for Rietveld refinement with PC and mainframe computers. See: Young, R. A.; Sakthivel, A.; Moss, T. S.; Paiva-Santos, C. O. *J. Appl. Crystallogr.* **1995**, *28*, 366.

**Table 3. Known Equilibrium Phases for Selected Metal Phosphides[a,b]**

| Fe/P | Ru/P | Co/P | Rh/P | Ni/P | Pd/P | Pt/P |
|---|---|---|---|---|---|---|
| $Fe_3P$ | $Ru_2P$ | $Co_2P$* | $Rh_2P$* | $Ni_3P$, $Ni_5P_2$ | $Pd_{15}P_2$, $Pd_6P$ | $Pt_5P_2$ |
| $Fe_2P$* | RuP* | CoP | $Rh_3P_2$ | $Ni_{12}P_5$, $Ni_2P$* | $Pd_{4.8}P$, $Pd_3P$ | $PtP_2$* |
| FeP | $RuP_2$ | $CoP_2$ | $Rh_4P_3$ | $Ni_5P_4$, $Ni_{1.22}P$ | $Pd_5P_2$*, $Pd_7P_3$ | |
| $FeP_2$ | $\alpha$-$RuP_4$ | $CoP_3$ | $RhP_2$ | NiP, $NiP_2$ | $PdP_2$, $PdP_3$ | |
| $FeP_4$ | $\beta$-$RuP_4$ | | RhP$_3$ | $NiP_3$ | | |

[a] Taken from *Binary Alloy Phase Diagrams*, 2nd ed.; Massolski, T. B., Ed.; ASM International: Materials Park, OH, 1990. [b] Metal/phosphorus stoichiometries of the molecular precursors **1a**−**7a** are underlined while metal/phosphorus stoichiometries of the nanocluster particulates in nanocomposites **1c**−**7c** are indicated with an asterisk.

formation of the metal phosphide/silica xerogel nanocomposites **1c**−**7c**. Microanalytical data indicate some loss of metal from the matrix during thermal treatment and some retention of phosphorus by the xerogel in excess of the amount required by the metal phosphide nanoclusters. As a control reaction, the bifunctional phosphine $L^B$ was incorporated into silica xerogel and was thermally treated at 750 °C under hydrogen for 3 h. Approximately 3.4% of the phosphorus originally loaded into the matrix is retained. The chemical nature of this retained phosphorus has not been determined.

Incorporation of the Os analogue of precursor **2a** into a silica xerogel matrix occurs as expected, but thermal treatment of the resulting molecularly doped xerogel gives a nanocomposite containing Os metal nanclusters. Not surprisingly, this Os(II) precursor is easily reduced by hydrogen to Os metal. The details of this reaction and the formation of several other metal/silica xerogel nanocomposites will be reported elsewhere.[30] Synthesis of an iridium phosphide/silica xerogel nanocomposite has been thwarted to date by the inability to prepare an Ir complex of sufficient chemical purity containing a bifunctional phosphine ligand. Ir analogues to precursor **4a** are obtained as brown oils.

Quite unexpectedly, though fortuitously, each dopant complex **1a**−**7a** serves as a single-source precursor to a single metal phosphide substance. As shown in Table 3, several equilibrium metal phosphide compositions are known for each metal investigated. Although the RuP and $PtP_2$ nanoclusters are formed from precursors having a M/P stoichiometry identical to that required for these metal phosphide phases, the other nanocluster stoichiometries require a relative loss of phosphorus from the corresponding molecular precursor during thermal treatment. While the M/P stoichiometry of the precursor does not generally control the M/P stoichiometry of the resulting nanoparticulate substance, the synthetic conditions employed here are selective for the formation of only one crystalline metal phosphide composition for each nanocomposite material. Phase separation into various metal phosphide compositions is not observed.

Although many of the metal/phosphorus phase diagrams are incomplete, the metal phosphide composition formed in most of these nanocomposites is that of the known congruently melting phase having the highest relative phosphorus content. This general observation holds for all of the nanocluster compositions formed except for that of nanocomposite **6c**. In the Pd/P phase diagram, $Pd_{4.8}P$ and $Pd_3P$ melt congruently, while $Pd_5P_2$ participates in a peritectic equilibrium at 852 °C. Interestingly, relative loss of phosphorus from precursor **6a** during thermal treatment would approach the $Pd_5P_2$ composition before reaching the $Pd_{4.8}P$ or $Pd_3P$ compositions.

We speculate that precursor complexes undergo reductive decomposition during thermal treatment producing incipient metal phosphide fragments. Phosphorus is lost from these incipient metal phosphide cores until either a congruently melting composition is reached or until a particularly stable stoichiometry, such as $Pd_5P_2$, is attained. Nanoparticle growth occurs through nucleation and growth mechanisms driven by diffusion, similar to those processes observed for CdS or CdSe cluster growth in silica glass.[31] The extent to which precursor M/P stoichiometry or the presence of a reactive gas during thermal treatment affect the final nanocluster composition requires much further study. Variation of these experimental factors might provide successful synthetic strategies for preparing selectively other metal phosphide substances as nanoparticulates, thus extending the general scope of this synthetic method.

**Acknowledgment.** C.M.L. thanks the donors of the Petroleum Research Fund, administered by the American Chemical Society, for partial support of this research and to support by, or in part by, the U.S. Army Research Office under grant number DAAH04-95-1-0146. We thank Dr. James E. Wittig for assistance in managing the TEM Facility within the Department of Applied and Engineering Sciences at Vanderbilt University and Dr. R. A. Young, School of Physics, Georgia Institute of Technology, for help in performing Rietveld refinement of the XRD pattern for RuP. We thank Ms. K. J. Burnam for experimental assistance.

**Supporting Information Available:** TEM micrographs, histograms of metal phosphide nanocluster particle-size distributions, powder XRD patterns, selected area electron diffraction data, and EDS spectra for all metal phosphide/silica xerogel nanocomposites (21 pages). Ordering information is given on any current masthead page.

CM970673P

(30) Carpenter, J, P.; Lukehart, C. M.; Milne, S. B.; Henderson, D. O.; Mu, R.; Stock, S. R. *Chem. Mater.*, submitted for publication.

(31) Liu, L. C.; Risbud, S. H. *J. Appl. Phys.* **1990**, *68*, 28.